InAs quantum dots grown on GaAs (100) surfaces subjected to novel in-situ treatments

V.H. Méndez-García
Instituto de Investigación en Comunicación Óptica and Facultad de Ingeniería,
Universidad Autónoma de San Luis Potosí,
Av. Karakorum 1470, Lomas 4^a Sección, San Luis Potosí, 78210 S.L.P., México,
Tel: +52 444 8250183, Fax: +52 444 8250198
e-mail: vmendez@cactus.iico.uaslp.mx

Recibido el 19 de enero de 2004; aceptado el 5 de abril de 2005

Novel in-situ treatments were performed to GaAs(100) surfaces in order to improve the size homogeneity of self-assembled InAs quantum dots (QDs). The treatments consisted in exposing the GaAs surfaces at high temperature for 10 seconds with the As_4- shutter closed. In the first experiment, the GaAs surface was just kept under no fluxes during 10 seconds, while in another growth the Si shutter was opened during the As_4 flux interruption. Both experiments were compared with a conventionally grown sample. Remarkable differences in the growth kinetics were observed when the InAs deposition was performed on different treated GaAs surfaces. The thermal treatment performed under no Si-flux extended the two to three-dimensional growth transition at much larger InAs thickness. On the contrary, the Si-treated sample showed an earlier lattice relaxation as compared with the reference sample. As for the final topology of the samples both treatments decreased the QDs diameter and height dispersion as compared with the conventionally grown sample. Therefore, a significant improvement on the size distribution of QDs was induced by the novel in-situ treatments, which also reduced the full width at half maximum (FWHM) of the photoluminescence (PL) emission spectra. Additionally, PL experiments showed a clear correlation between the dots size increase and the emission peak redshift observed for the QDs grown on GaAs surfaces subjected to the different treatments.

Keywords: Nanoestructures; quantum dots; molecular beam epitaxy; semiconducting III-V materials.

Novedosos tratamientos fueron realizados in-situ a superficies de GaAs (100) con el propósito de obtener una mayor uniformidad en los tamaños de los puntos cuánticos (QDs) autoensamblados de InAs. Los tratamientos consistieron en exponer las superficies de GaAs a temperatura alta por 10 segundos con el obturador de As_4 cerrado. En un primer experimento la superficie de GaAs únicamente se mantuvo a 650°C sin ningún flujo, mientras que en el otro crecimiento el obturador de Si se abrió durante la interrupción del flujo de As_4. Ambos experimentos se compararon con una muestra crecida convencionalmente. Notables diferencias fueron observadas en la cinética de crecimiento cuando el depósito de InAs se realizó sobre las diferentes superficies tratadas de GaAs. El tratamiento térmico realizado sin flujo de Si extiende a mucho mayor espesor la transición del crecimiento bidimensional a tridimensional de InAs. Por el contrario, la muestra tratada con Si mostró más tempana relajación de red comparada con la muestra de referencia. Respecto a la topología final de las muestras, ambos tratamientos redujeron la dispersión en alturas y diámetros, respecto a la muestra crecida convencionalmente. Por lo tanto, un significativo mejoramiento fue inducido por los tratamientos térmicos en la distribución de tamaños de los QDs, lo cual a su vez redujo el ancho medio (FWHM) de los espectros de fotoluminiscencia (PL). Además, los experimentos de PL mostraron una clara correlación entre el aumento en los tamaños de los puntos y el corrimiento hacia el rojo del pico de emisión que se observó para los QDs crecidos sobre las superficies de GaAs sometidas a los diferentes tratamientos.

Descriptores: Nanoestructuras; puntos cuánticos; epitaxia por haces moleculares; materiales semiconductores III-V.

PACS: 81.07.Ta; 81.16.Dn

1. Introduction

Nowadays, one of the major goals on semiconductors research field is the development and optimization of zero-dimensional structures where the 3D quantum confinement imposed on the electron and on hole motion leads to strongly modified electronic and optical properties [1-3]. These zero-dimensional structures also known as quantum dots (QDs) should significantly improve today devices performance based on quantum well technology, as well to contribute to the development of new optical devices [4,5]. QDs self-assembling by employing the Stranski-Krastanov (S-K) growth mode of highly strained systems, particularly InAs on GaAs substrates, has been pointed out as one of the most promising ways to achieve coherent three-dimensional confinement structures. Basically, in this growth mode a thin film of one crystal is deposited on the surface of another crystal. The two crystals belong to the same symmetry group, have different lattice constants, and form a coherent interface when the deposited film is thin enough. The lattice mismatch induces an elastic field. In order to lower the elastic energy, the film breaks into islands. The islands grown this way are usually uneven in size and spatial arrangement. The quantum dots size nonuniformity causes a spread in the electronic energy emission levels of samples, which limits its application to potential devices and complicates the succeeding fundamental physics studies. Several groups have sought a tight control of the uniformity, size, density, and location of self-

assembled QDs through:

(i) depositing the dots employing growth rates as low as 0.02 monolayers (ML) per second [6];

(ii) using alternating group-III and group-V fluxes, the so-called atomic layer epitaxy (ALE) method [7];

(iii) changing growth parameters such as substrate temperature and V/III flux ratio [8,9]; and

iv) making growth interruptions after QDs formation [10].

Despite these intense efforts, it remains a challenge to fabricate uniform QDs arrays by the S-K growth mode.

In this article, we propose two in-situ procedures to improve the size distribution of the dots' arrays. Our approach is to subject the GaAs buffer layers to annealing processes at high substrate temperature under a Si flux and under no flux during a short time interval before the InAs QDs growth. The annealing process of the GaAs surfaces leads to a Ga surface that could change the chemical status of the substrate prior to the InAs deposition. Besides, Si atoms were employed in order to alter the elastic field at the InAs/GaAs interface since it is well known that the lattice mismatch between InAs and Si is $\sim$11.5%, whereas the lattice parameter difference between InAs and GaAs is about 7%; thus the mechanism of self-assembling would certainly be affected in some way. The atomic force microscopy (AFM) images showed evidences of improved morphology and size dispersion for the InAs QDs grown on GaAs surfaces subjected to the treatments. Consequently, PL emission spectra of treated samples showed narrower linewidths and a redshift in the emission peak due to the QDs size increase.

2. Experimental

GaAs (100) substrates previously etched in an H_2SO_4: H_2O_2: H_2O (5:1:1) solution were loaded into a RIBER-32 MBE system. Once the substrate native oxide layer was removed by thermal desorption at 585°C under arsenic molecular beam flux in ultra high vacuum environment, a 0.5 μm-thick GaAs buffer layer (BL) was grown at 600°C in all samples at the growth rate of 0.5μm/hr. After that, we prepared three different kinds of samples.

1) Sample M1 was prepared conventionally depositing the equivalent to 2.1 ML of InAs directly on the GaAs substrate surface at 500°C employing a growth rate of 0.1 ML/sec.

2) For Sample M2, after the growth of the GaAs BL the substrate temperature was increased up to 650°C under As_4 flux. Then, simultaneously, the As_4-shutter was closed and the Si-shutter was opened at this temperature for 10 seconds. The As_4-flux was reestablished after 10 seconds, and the Si-shutter was closed. Immediately after that, the substrate temperature was lowered down to 500°C and, like for sample M1, 2.1 ML of InAs were deposited.

3) Sample M3 was prepared following the same procedure employed for sample M2, except that during the time interval of 10seconds the Si-shutter was not opened. Only the As_4 overpressure was interrupted at 650°C for this sample (the MBE growth chamber background pressure was observed to be 8.2×10^{-8} Torr). The InAs equivalent thickness was 3.4 ML for sample M3.

It is worth making a remark that for samples M1 and M2, we observed the 2D-3D transition referring to reflection high-energy electron diffraction (RHEED) patterns at 1.7 ML, while for sample M3 it was observed up to 3.0 ML of InAs. Therefore, for all samples, we stopped depositing InAs 0.4 ML after the relaxation process took place. The samples surface was characterized by atomic force microscopy (AFM) in air, and 15 K-PL measurements were performed with a 514 nm wavelength Ar laser as the excitation source.

3. Results and Discussion

The behavior of the RHEED specular beam intensity along [011] azimuth observed during the GaAs surface treatment at 650 °C is shown in Fig. 1. The inset shows the intensity profiles from the RHEED patterns observed at different stages of the GaAs surfaces treatment. It is important to mention that the RHEED patterns showed an As-rich 2×4 surface reconstruction all through the GaAs buffer layer growth and just before the high-temperature treatments were performed at 650°C. The arrows in the left hand side inset of Fig. 1 show some of the 1/4-order reconstruction streaks, characteristic of the [011] azimuth of GaAs. When the As_4 shutter was closed, the specular beam intensity increased abruptly and the $4\times$ reconstruction changed to a blurred $1\times$ RHEED pattern. Immediately after the As_4 flux was reestablished again, the intensity dropped and the $4\times$ pattern was recovered with higher intensity than the observed just before the treatment. In particular it was observed an increase in the intensity of the diffraction rods $(0\bar{1})$, (00), and (01) as well as narrower 1/4-order reconstruction streaks as is shown by the corresponding RHEED intensity profile in the right hand side inset of Fig. 1. On the other hand, the RHEED pattern along the $[0\bar{1}1]$ azimuth experienced only haziness of the half order reconstruction. It is worthy of notice that the former RHEED behavior, observed when the As_4 shutter was closed, was almost identical for both thermal treatments (with and without Si). Moreover, the RHEED patterns obtained at the end of the treatments were roughly the same. Therefore, the observed changes are mainly attributed to the As evaporation from the surface since, at a temperature of 650°C, the As evaporation rate is so elevated that it leaves a large number of vacancies and could have let the underlying Ga

exposed [11]. Actually, the (2×1) surface reconstruction observed during the thermal treatments has been associated to a Ga-rich reconstruction, which leads to nonmetallic and nonpolar surface [12]. The above discussion is very important in our experiments because the nonpolarity not only involve the existence of As free bonds during the thermal treatment which could propitiate As-Si binds for Sample M2 growth, but also suggest the creation of droplets on the surface due to the high surface tension of the Ga atoms. At the moment the As_4 shutter was reopened, no oscillations of the specular beam intensity were observed indicating that there was no GaAs overgrowth. Thus, Si atoms bonded to As (for M2) and Ga droplets could have rested on the surface prior to the InAs deposition, contributing in this way to the remarkable changes observed for these QDs as will be explained later.

Figure 2a shows the RHEED specular beam intensity oscillations observed along the [011] azimuth when the InAs deposition was performed on the sample grown under standard conditions (Sample M1). At the initial stages of growth (below ∼1.5 ML), the oscillations obtained from the specular beam indicated a layer-by-layer growth regime and a somewhat diffuse and streaky 1× diffraction pattern was observed. When the specular beam intensity dropped as a consequence of the decrease of the 2D diffraction features, the RHEED pattern evolved into a strongly spotty pattern indicating that 3D islands had developed on the surface [13].

Figure 2b shows the oscillations of the specular beam obtained on [011] direction when the InAs growth was performed on Sample M3, the sample subjected to high temperature under no fluxes. Conversely to sample M1, the RHEED specular beam intensity showed a periodic oscillatory behavior indicating a layer-by-layer growth. The RHEED pattern (not shown) obtained at the end of the growth of 2.1ML was still streaky, an additional evidence of the InAs bidimensional growth. After the deposition of 2.1 InAs ML the growth was interrupted during 40 seconds under As_4 flux in order to observe the RHEED patterns on several azimuths. Streaky RHEED patterns were observed along all the azimuths. Then, the InAs deposition was continued until we observed the 2D-3D transition. The change in the diffraction pattern from streaky to spotty took place after the deposition of 3.0 InAs ML, although the growth was interrupted 0.4 ML further. It is worthy of notice that this experiment was corroborated a number of times.

The prolongation of the InAs bidimensional growth regime on Sample M3 is rather surprising since without the

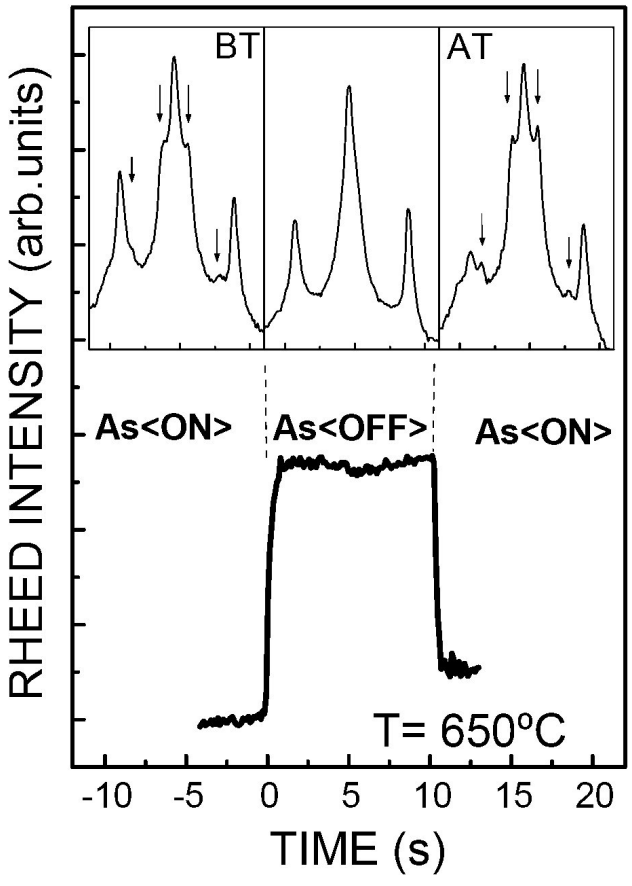

FIGURE 1. RHEED specular beam intensity behavior observed along [011] azimuth when the As_4 cell shutter was closed at 650°C. The inset shows the intensity profiles taken from the RHEED patterns observed at different stages of the GaAs surface treatments: before the treatment, when the As_4 shutter was closed, and after the treatment.

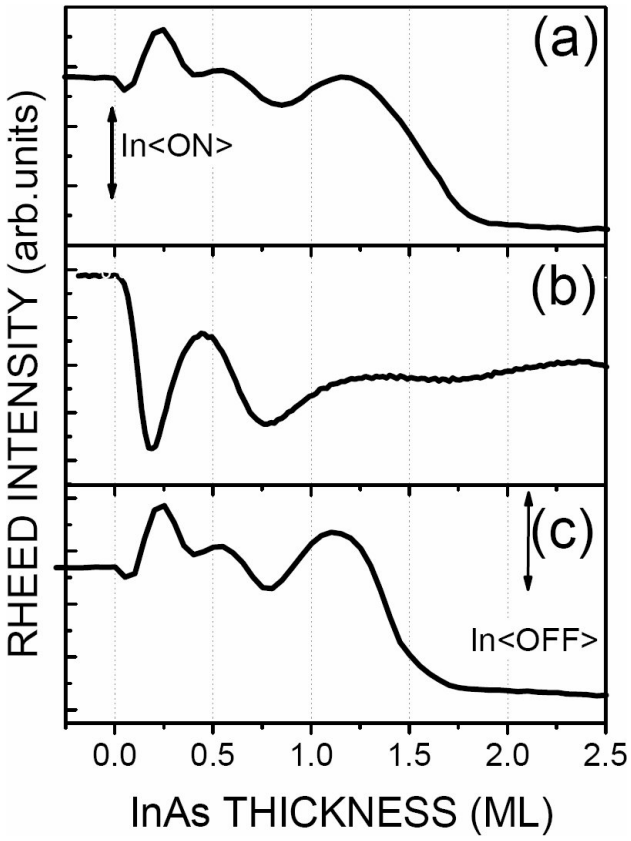

FIGURE 2. Specular beam intensity oscillations obtained along [011] azimuth during the InAs growth of (a) Sample M1, (b) Sample M3, and (c) for Sample M2.

use of surfactants, and growing InAs under As-stable conditions the island formation was delayed. The delay could be explained considering that both, lattice strain and the balance between surface, as well as interface, and the film free energies determine the growth mode of the film. One of the conditions for the epitaxial film to wet the substrate is set by the inequality $\sigma_s > \sigma_f + \sigma_i$, where σ_s, σ_f and σ_i are the substrate free energy, epilayer surface energy and interface energy, respectively [14]. If the inequality is satisfied, the layer-by-layer or Frank-Van der Merwe (F-M) growth mode occurs. On the other hand, if the inequality has the opposite sign, the film will usually follow the Volmer-Weber growth, *i.e.*, no wetting of the substrate. Finally, the Stranski-Krastanov (S-K) growth mode takes place when there is a wetting of the substrate surface, but the overlayer strain is unfavorable for sustaining the F-M growth mode, as in the InAs/GaAs growth. When the thermal annealing process was performed, As_4 evaporation from the topmost layers occurred, as confirmed by the (2×1) RHEED pattern. It has been reported that severe As-desorbtion could result on atomically rough surfaces [15]. This atomically rough surface could be seen as a dangling-bonds rich plane that contributed to increase the substrate free energy σ_s, satisfying in this way the previous inequality. Furthermore, the formation of Ga droplets on these surfaces reduced the effective lattice mismatch δ_{eff}, the driving force for quantum dot formation. Remembering that δ_{eff}= (1-X_{Ga})δ_{InAs}, where X_{Ga} is the Ga content, in this case provided by the As desorbtion, and δ_{InAs} is the InAs/GaAs mismatch. Therefore, the surface obtained after the deposition of 2.1 ML of InAs exhibited the F-M growth mode as a consequence of large σ_s and of the diminution of δ_{eff}, propitiated by the thermal treatment. Once the InAs deposition continued on this flat surface, there was a gradual increase in the overlayer strain and the relaxation took place through the nucleation of new-fangled islands, as will be seen by the AFM images.

On the other hand, Fig. 2c shows the RHEED specular beam intensity oscillations during InAs deposition for sample M2, thermal treatment plus Si-flux. In Sample M1, the enhancement of the surface roughness associated with the formation of 3D islands occurs at 1.7 ML, in good agreement with other publications [9,16], but for sample M2 it happens at 1.5 ML suggesting an earlier lattice relaxation. Moreover, this result was found to be independent of the InAs growth rate, which was varied in a series of experiments from 0.1 to 0.7 ML/sec. Always the InAs lattice relaxation was observed sooner for the Si-treated samples than for the conventionally grown ones. The role of Si on the early nucleation of islands will be discussed later on.

Note that, despite the great similarities observed during the thermal treatments of Samples M2 and M3 (in particular the As-evaporation at 650°C), the initial stages of InAs growth were quite different for both samples. This indicates that Si atoms are playing an important role on Sample M2.

The AFM images of the grown samples are shown in Fig. 3 with a scan size of 0.8×0.8 μm^2 and a vertical scale equivalent to 15 nm. Fig. 3a shows the islanded surface obtained from Sample M1, where the InAs deposition was performed employing the conventional procedure. The small dots exhibit a density of 15×10^{10} cm^{-2} with a random size distribution, which is a usual characteristic of the Stranski-Krastanov growth mode. On the other hand, Fig. 3b shows the AFM image of Sample M3 obtained after depositing 3.4 InAs ML. It is evident that a significant improvement in the island size distribution has taken place. Although the dots are still distributed randomly, they exhibit the biggest uniformity as well as the largest dimensions of all the growths performed. The AFM statistics will be discussed in the next paragraph. The dots density is around 5×10^{10} cm^{-2}. Obviously, the new dots morphology resulted from the thermal treatment at which the GaAs surface of Sample M3 was subjected since QDs formation is strongly influenced by the early steps of growth, as previous reports affirm [17]. On the other hand, Fig. 3 shows the InAs QDs grown on the GaAs surface subjected to the thermal treatment under a Si flux. The dots exhibited bigger dimensions, a reduction in their density ($\sim9.8\times10^{10}$ cm^{-2}) as well as a better arrangement compared with the QDs grown under standard procedures. Evidently, the Si atoms deposited on the GaAs surface of Sample M2 have played an important role in the singular QDs arrangement obtained for this sample. Recently, *Quian et al.* [18] reported a model where the Si atoms act like nucleation centers in the QDs formation by reducing the strain for the incoming In atoms due to they exhibit a smaller radius (r_{Si}= 1.17 Å) than the In atoms (r_{In}= 1.62 Å). *Quian* explained that when the Si atoms are incorporated into the wetting layer occupying the position of an In atom, they relax the strain of those atoms close to the Si positions. Therefore, as new In atoms arrive they find energetically more favorable to nucleate on those places where their presence do not generate greater additional energy, *i.e.*, close to the Si-strain-relieved regions. Since we employed a Si dopant cell we had a relatively low quantity of Si atoms on the GaAs surface, about 8.3×10^{11} Si atoms per cm^2. Therefore, the scheme of Si incorporation into the InAs wetting layer is rather allowed, propitiating preferential places for the additional InAs to be nucleated on and driving to a reduction of the dots density.

It is worthy of remark that the InAs wetting layer thickness obtained for Samples M1 and M3 was about 1ML while for Sample M2 was less than 0.5ML, considering a parabolic QDs shape with the dimensions obtained by AFM. These results imply that the self-assembling process was very similar for Samples M1 and M3, it's like they had followed the S-K growth mode. On the contrary, for Sample M2 the mechanism of QDs formation could have been different supporting the idea of formation of islands helped by Si-nucleation centers. In order to get an accurate measurement of the wetting layer from the samples and additional information about the QDs nucleation, further experiments like transmission electron microscopy (TEM) are necessary and are currently in progress.

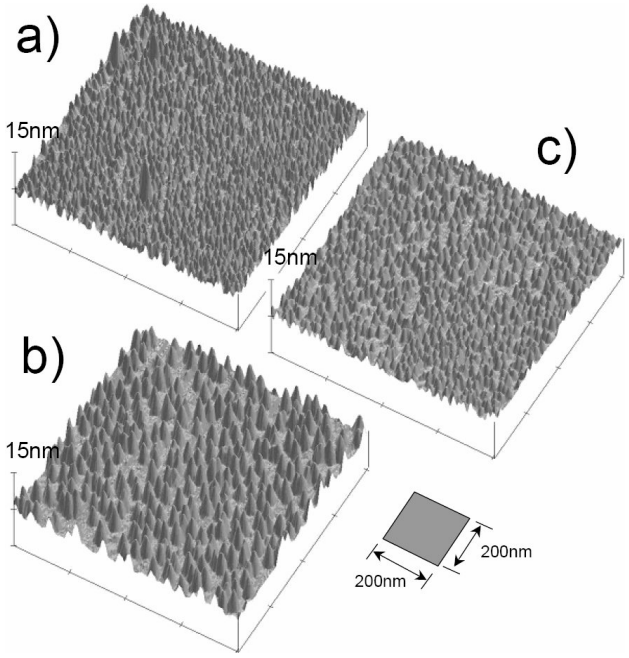

FIGURE 3. AFM images obtained after the growth of InAs QDs on (a) a conventional GaAs surface, (b) a GaAs surface subjected to a thermal treatment under no fluxes, and (c) a GaAs surface exposed to a Si flux during a thermal treatment.

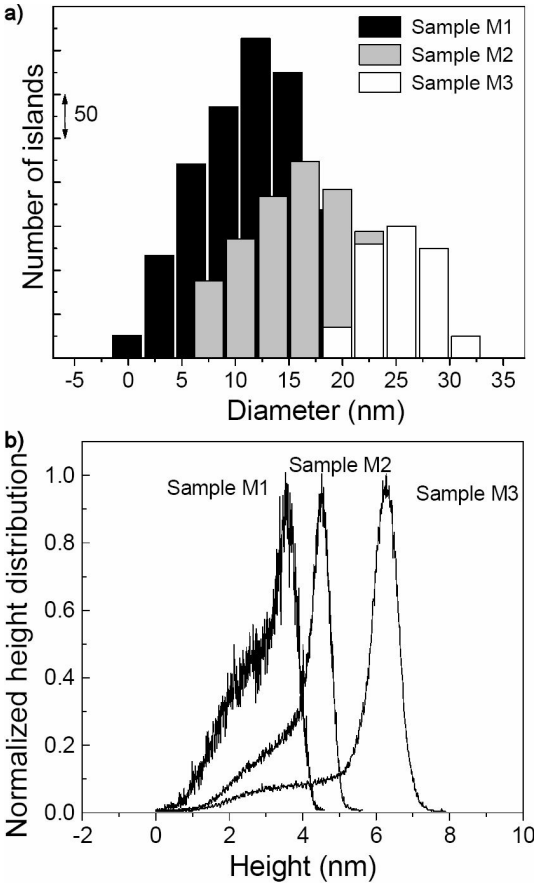

FIGURE 4. QDs statistics obtained by AFM for the resultant QDs surfaces, (a) diameters histograms, and (b) Heights distributions.

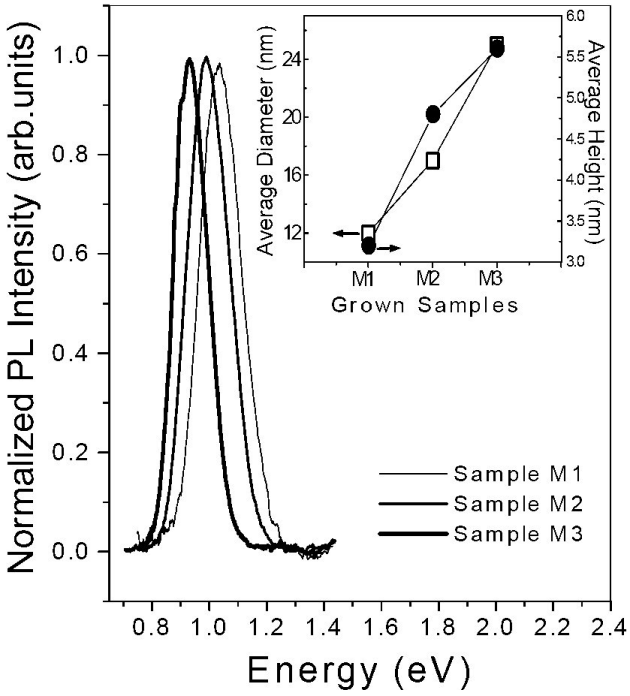

FIGURE 5. Photoluminescence spectra obtained at 15 K for the three experiments performed. Inset shows a plot of the average dimensions obtained for the QDs.

Figure 4 shows the QDs statistics as obtained by AFM. The island diameter histograms are shown in Fig. 4a while height distributions are shown in Fig. 4b. The diameters histograms show clearly how the increase of the dots dimensions is accompanied by a diminution in the dots' density. QDs grown employing the typical procedure had an average height of 2.9±1 nm, and diameters about 12±3.1 nm. Meanwhile, the dots grown on the GaAs surface, annealed under a Si flux, observed an increase in their sizes resulting with heights around 4.3±0.8 nm and average diameters of 17±4 nm. However, the largest dots were those grown on the GaAs surface annealed at high-temperature under no flux with an average height of 5.9±0.5 nm and diameters about 25±2.5 nm. The standard deviations of the former parameters are taken as a half of the FWHM of the Gaussian fits performed to the curves of Fig. 4. It is observed that the relative diameter and height dispersion changed from above 26% for sample M1, to below 10% for sample M3. The former improvements on the QDs size was reflected on the PL emission of QDs as is shown in the next paragraph.

The PL spectra from samples at 15 K are shown in Fig. 5. It can be seen that the QDs emission peak is centered around 1.03, 0.98 and 0.93 eV for Samples M1, M2 and M3, respectively. The inset shows a relation of the dots average dimensions as obtained by AFM for the different grown samples. It is evident that the gradual increase of the dots' sizes matches perfectly with the gradual redshift observed in the PL spectra. Moreover, it was found that the redshift magnitude depends on both, the high temperature treatment exposure time as well as on the amount of InAs deposited. Thus, these results sug-

gest the possibility of tailoring the QDs emission peak by changing the growth parameters. Additional experiments directed toward the manipulation of the red shift emission by employing the thermal treatments are currently under investigation. If achieved, this method would open new possibilities in the synthesis of lower frequency emitting devices based on QDs. Note that the emission wavelength of the treated samples is close to $\sim$1.3μm, the wavelength where optical dispersion and lessening are minimized in optical data transmission systems. On the other hand, it was observed a reduction in the FWHM of the PL emission spectra of Sample M3 as a consequence of the size uniformity improvement of the QDs grown on the GaAs surfaces annealed at high-temperature.

4. Conclusions

Novel in-situ thermal treatments were performed to the GaAs surfaces before the InAs deposition. The high temperature treatment performed under no flux affected considerably the first stages of InAs deposition since the 2D-3D transition occurred at a thicker film thickness than the observed for the other samples. On the other hand, it was observed that Si atoms acted as nucleation centers in the QDs formation inducing a faster lattice relaxation and modifying the dimensions as well as the arrangement of the InAs QDs. Moreover, the resultant InAs QDs after applying both treatments showed a considerable improvement on their arrangement as well as a significant reduction in their size dispersion. The increase of the dots' dimensions and size homogeneity was revealed as an energy redshift as well as in narrower PL emissions for the dots grown on the GaAs surfaces subjected to the different thermal treatments.

Acknowledgments

The authors would like to express their thanks for the laboratory facilities provided by Dr. Alfonso-Lastras, Dr. A.Yu. Gorbatchev and the technical support from B.E. Torres-Loredo, J.G. Nieto-Navarro and E. Ontiveros. This work was partially supported by CONACyT-Mexico, FAI-UASLP, PROMEP-SESIC.

1. Y. Arakawa and H. Sakaki, *Appl. Phys. Lett.* **40** (1982) 939.
2. M. Grundmann, O. Stier, and D. Bimberg, *Phys. Rev. B* **52** (1995) 11969.
3. A. Wojs, P. Hawrylak, S. Fafard, and L. Jacak, *Phys. Rev. B* **54** (1996) 5604.
4. D. Pan, E. Towe, and S. Kennerly, *Appl. Phys. Lett.* **73** (1998) 1937.
5. J. Phillips, K. Kamth, T. Brock, and P. Bhattacharya, *Appl. Phys. Lett.* **72** (1998) 3509.
6. P.B. Joyce *et al.*, *Phys. Rev. B* **64** (2001) 235317.
7. D.L. Huffaker and D.G. Deppe, *Appl. Phys. Lett.* **73** (1998) 520.
8. P.B. Joyce *et al.*, *J. Crystal Growth* **227-228** (2001) 1000.
9. G.S. Solomon J.A. Trezza, and J.S. Harris Jr., *Appl. Phys Lett.* **66** (1995) 3161.
10. S. Kiravittaya, Y. Nakamura, and O.G. Schmidt, *Physica E* **13** (2002) 224.
11. M. López, Y. Takano, K. Pak, and H. Yonezu, *Jpn. J. Appl. Phys.* **31** (1992) 1745.
12. D.J. Chandi, *J. Vac. Sci. Technol. A* **5** (1987) 1482.
13. C.W. Snyder, B.G. Orr, D. Kessler, and L.M. Sander, *Phys. Rev. Lett.* **66** (1991) 3032.
14. D.J. Eaglesham and M. Cerullo, *Phys. Rev. Lett.* **64** (1990) 1943.
15. C. Orme, M.D. Johnson, J.L. Sudijono, K.T. Leung, B.G. Orr, *Appl. Phys. Lett.* **64** (1994) 860.
16. P.B. Joyce, T.J. Krzyzewski, G.R. Bell, B.A. Joyce, and T.S. Jones, *Phys. Rev. B* **58** (1998) R15981.
17. B.F. Lewis *et al.*, *J. Vac. Sci. Technol. B* **2** (1984) 419.
18. Z. Quian *et al.*, *J. Cristal Growth* **200** (1999) 603.